JOURNAL OF MATERIALS SCIENCE: MATERIALS IN MEDICINE 9 (1998) 485–492

Bioactivity modulation of bioactive materials in view of their application in osteoporotic patients

M. MATTIOLI BELMONTE*, A. De BENEDITTIS, R. A. A. MUZZARELLI, P. MENGUCCI, G. BIAGINI
CIBAD-Centre for Innovative Biomaterials, School of Medicine, University of Ancona, Via Tronto 10/A, 60020 Ancona, Italy

M. G. GANDOLFI, C. ZUCCHINI
Institute of Histology and Embryology, University of Bologna, Via Belmeloro 8, 40126 Bologna, Italy

A. KRAJEWSKI, A. RAVAGLIOLI, E. RONCARI
Institute for Technological Research on Ceramics, Italian National Research Council, C.N.R., Via Granarolo 64, 48018 Faenza (RA) Italy

M. FINI, R. GIARDINO
Experimental Surgery Department, Research Institute Codivilla - Putti Rizzoli Orthopaedic Institute, University of Bologna, Via di Barbiano 1/10, 40136 Bologna, Italy

The application of bioactive ceramic coatings to prostheses confers strength to a material (ceramic or biological glass) that exerts beneficial effects on bone-tissue growth but that itself lacks the toughness and stability required of an implant device. The rate of bioactivity is related to the chemical reactivity of the material and causes interface dissolution, precipitation and ion-exchange reactions. Ceramics may differ in sintering temperature and thus exhibit differences in their *in vitro* dissolution features and *in vivo* performance. To test these effects, *in vitro* and *in vivo* studies were carried out on two biocompatible biological glasses and a ceramic of proven bioactivity in view of their potential utilization as covering materials. In addition, a modified chitosan was adsorbed on the surface of a series of hydroxyapatite (HA) samples. Human fibroblasts and/or osteoblasts were used for the *in vitro* tests, and normal (INT) and osteoporotic (OVX) rats, normal rabbits and sheep for the *in vivo* studies. Similar chemical changes were observed in both glasses, suggesting that these materials underwent modifications directly dependent on their biological environment. The *in vivo* tests point to the possibility of improving the bioactivity of ceramic substrates with chitosan. However, the different behaviour of the materials *in vitro* and *in vivo* suggests that these tests should be conducted in parallel.

1. Introduction

Metal alloy implants have been in use in orthopaedic surgery for several decades because of their excellent mechanical properties. Over the past few years, researchers have been trying to improve on this merely mechanical approach and to develop a new series of materials that can guarantee not only superior mechanical performance but also an excellent biological response. To this purpose, several different materials have been produced to meet almost every conceivable need, yet not all the problems connected with these implants have been solved, such as distance cell migration, breakage, stress shielding, reactivities and growth restriction. A number of bioresorbable polymer devices now offer valid alternatives for some indications, but even though cell adhesion has a fundamental role in implant viability, these devices have one essential drawback in the inherently lower strength of such polymers compared with metals [1]. Nonetheless, Ca-phosphate ceramics are currently used as cancellous-bone graft substitutes, and several patients with traumatic impressions of the tibial plateau treated with hydroxyapatite or tricalcium phosphate have experienced complete integration of the ceramic without adverse reaction [2, 3].

The biodegradation of ceramics is performed *in vivo* by monocytes and multinuclear cells (osteoclasts). At the physiological pH, the solubility of Ca-phosphate ceramics depends mainly on their physico-chemical characteristics. In particular, solubility increases

* Author to whom correspondence should be addressed.

0957–4530

as the chemical composition of the ceramic shifts towards the exact hydroxyapatite (HA) stoichiometry. It is well known that the implantation of a material induces an inflammatory reaction and that monocytes are the first cells to be mobilized at the implant site during this reaction. As a consequence, the physiological fluids around the implant change in protein composition and a lowering of the pH is commonly observed. In these conditions, the stability of Ca-phosphate decreases, and interactions between the proteins and the surface of the ceramic change in relation to pH variation.

Several ultrastructural studies have investigated the specific behaviour of monocytes towards a Ca-phosphate ceramic [4]. When exposed to protein solutions, the surface of a bioactive Ca-phosphate ceramic undergoes quick chemical changes. Dissolution mechanisms and protein interactions at the bone–implant interface have been observed, and the net loss of phosphate ions from the surface has been shown to be slower in tests with phosphate buffer saline compared with alpha-minimum essential medium (MEM) solutions [4, 5].

Investigations of the dissolution–reprecipitation phenomena involved in the formation of the hydroxyapatite–bone bond have identified two joining modes [6]:

1. bone tissue components bonded to HA through a recrystallization zone similar in structure to the reprecipitation layer observed in corrosion assays, and
2. bone tissue components bonded directly to HA crystals with no morphologically discernible signs of dissolution.

Orthopaedic endoprostheses need to be firmly fitted to the bone. In cementless devices, this fit has to be achieved by the functional integration of the prosthesis with the surrounding bone. The integration process is influenced by several factors, among which are the type of implant material and the initial fit of the device. Cell adhesion to the biomaterial plays a fundamental role. Recently, it has been reported that the extracellular matrix (ECM) is a powerful regulator of cell adhesion and indeed cells respond to the ECM by means of integrins, which couple the components of the ECM with the actin cytoskeleton. This structure thus mediates adhesion to the ECM and therefore to the implant material. In this respect, the possibility of bonding osteoinductive polymers such as modified chitosans [7, 8] to the ceramic substrate could enhance cell proliferation and consequently anchorage to the implant.

To test these effects, *in vitro* and *in vivo* studies were performed on two different bioactive systems: biological glasses (AP40 and RKKP, differing only for the presence of dopants) and HA (adsorbed or not with modified chitosans). Human fibroblasts and/or osteoblasts were used for the *in vitro* test in order to verify if cells with different specialization could affect the modification of the materials differently. Normal (INT) and osteoporotic (OVX) rats, normal rabbits and sheep were utilized for the *in vivo* studies.

TABLE I Original chemical composition of the biological glasses (wt %)

Element	AP40[a]	RKKP[a]
Ca	45.38	44.65
P	8.68	7.89
Si	36.54	36.10
Na	6.06	5.94
Mg	3.04	2.96
K	0.30	0.28
La	–	0.75
Ta	–	1.43

[a] Fluorine content of anionic partners: 5.57 wt % in AP40 and 5.56 wt % in RKKP; the remainder to 100 is oxygen.

2. Experimental procedure

2.1. Materials

Two types of biological glass, AP40 and RKKP, which were silico-phosphates of Ca, K and Na, were used. They have a similar composition (Table I) and differ only for the presence of some amphoteric network-formers (La^{3+} and Ta^{5+} in RKKP), which contribute to stabilize their molecular network, and have less side-effects than Al^{3+}. Prototypes of plaques and nails 2 mm in diameter made with these biological glasses were prepared for the *in vitro* and *in vivo* tests, respectively.

HA powders were synthesized by the mechano-chemical method [9–11]: reactive grinding was performed in Teflon containers using ZrO_2 balls by wet milling of a slurried mixture of $CaHPO_4 \cdot 2H_2O$ and $CaCO_3$ in proportions that would yield the desired Ca : P atomic ratio of 5 : 3 (or 1.667). Plaques and nails made of commercial salts and prepared according to traditional criteria were used as controls. Prototypes of HA plaques and nails (2 or 3 mm in diameter) were obtained by slip-casting and pressing of the powders. The HA samples for implants made with commercial powders were fired at 1280 °C; those obtained by mechano-chemical reaction were fired at 1250 °C. Flexural strength tests of the nails, carried out on a four-point device, gave values of 50 and 150 MPa, respectively. Before testing, plaques and nails were sterilized at 120 °C.

N,N-Dicarboxymethyl chitosan (DCMC), that has been fully characterized both chemically and enzymatically [12] was used. HA nails were immersed into a filtered chitosan solution, kept under vacuum for 6 h to remove adsorbed gas, and dried in a vacuum oven at 60 °C overnight to obtain chitosan-coated HA (CcHA). DCMC was also associated with calcium and phosphate (CaP, Gentili) to obtain DCMC–CaP, a soft and spongy hydrophilic material. The final products were sterilized by γ-ray irradiation at 25 J kg^{-1}.

2.2. Cell cultures

In vitro cell-growth tests were performed on the two biological glasses, HA and CcHA, using human fibroblasts and osteoblasts. Cells were seeded at a density of 50 000 per well in wells containing the material to be tested. Cultures were kept in a thermostatic

device at 37 °C in a 5% CO_2 atmosphere for seven days. Cell proliferation and adhesion were evaluated using phase-contrast light microscopy and scanning electron microscopy (SEM).

2.3. Animals

Of the 20 adult female Sprague–Dawley rats, ten were bilaterally ovariectomized four months before implant surgery (OVX rats). HA or biological-glass nails were implanted bilaterally in the femoral condyles of INT and OVX rats. The animals were sacrificed two months later and the condylar region with the implant removed for histological examination.

Under general anaesthesia, the femoral condyles of six adult male New Zealand rabbits (3 ± 0.25 kg) were exposed by a lateral longitudinal incision. In each condyle, a substance defect (2.9 mm in diameter) was made in a central position, 1 cm above the trochlear apex, for transversal insertion of a CcHA nail. The animals were sacrificed two months after surgery and the femurs removed for histological examination.

Sheep were treated according to the recommendations of the European Union and fed a standard diet. A bone defect was made in the femoral epiphyses with a 6-mm drill. During this procedure the holes were carefully rinsed with 0.9% NaCl solution and cleaned out to remove abraded particles, reduce drilling temperature and avoid bone necrosis. In the right leg, the hole was completely filled with DCMC–CaP, while the hole in the left leg was left unfilled to serve as a control. Animals were killed under general anaesthesia after 40 and 60 days. The femurs were removed and sawn to produce fragments for histological examination.

2.4. Histological processing

All specimens were fixed in 10% buffered formalin, dehydrated in an ascending series of alcohols and embedded in metacrylate resin. After polymerization, blocks were sectioned along a plane perpendicular to the bone surface with a diamond saw to obtain undecalcified 80–100 μm thick ground sections. After Masson–Goldner and von Kossa staining, they were examined histologically for cellular and stromal content.

2.5. Scanning electron microscopy and microanalysis

Methylmetacrylate-embedded slices 200 μm in thickness were mounted onto stubs with colloidal graphite, coated with carbon for vacuum evaporation and observed with a Philips XL 20 SEM equipped for X-ray microanalysis (EDX, EDS-PV 9800).

Rat specimens were first observed by back-scattered electron imaging, then subjected to X-ray analysis. Operative conditions for the analysis were: voltage, 25 kV; magnification, × 400; counts per second (c.p.s.), no less than 2000; tilt angle, 15°; time count, 250 s. Only the K_α values of each element were considered, and the semiquantitative per cent concentrations were calculated using ZAF (Z = atomic number, A = adsorption; F = fluorescence) procedure correction. To assess whether the different metabolic conditions affected the materials differently, in each animal sample the centre of the implant and the bone surrounding it were subjected to X-ray microanalysis.

3. Results

3.1. *In vitro* studies

The semiquantitative data from phase-contrast light microscopy and SEM are summarized in Table II.

3.1.1. Biological glasses

Fibroblasts cultured on AP40 and RKKP plaques appeared flattened and exhibited long projections towards the porosity of the material. Cell growth was greater for RKKP (Fig. 1).

Similarly, at light microscopy *osteoblasts* evidenced better growth round RKKP (Fig. 2), while SEM analysis showed a nearly complete absence of cells on AP40 and sparse clusters on RKKP.

3.1.2. HA

Fibroblasts exhibited good growth, with very flat cells displaying a tendency to penetrate the porosity of the ceramic (Fig. 3). *Osteoblasts* grew uniformly, with cells that appeared very flat.

3.1.3. Chitosan–coated HA (CcHA)

Fibroblast growth was scarce. For this reason, a study of osteoblast growth was not performed.

3.2. *In vivo* studies

3.2.1. Biological glasses

The morphological study of the AP40 implant in OVX rats demonstrated the presence of a fibrotic reaction and scarce osteoinduction (Fig. 4). With SEM, osteoinduction appeared moderate both in INT and OVX rats (Fig. 5). Light-microscopic analysis showed greater osteoinduction at the bone–RKKP interface in OVX rats (Fig. 6). This observation was confirmed by the presence of a greater number of osteointegration *foci* observed by SEM with RKKP (Fig. 7). The results of the EDX microanalyses performed at the centre of

TABLE II Semiquantitative evaluation of cell growth[a] (SEM analysis)

	AP40	RKKP	HA	CcHA
Fibroblasts				
Cell growth				
Round the material	+	+ +	+ + +	+ ±
On the material	±	+	+ + +	±
Osteoblasts				
Cell growth				
Round the material	+	+ ±	+ + +	NE
On the material	− / ±	±	+ + ±	NE

[a] (−) negative, (±) insufficient, (+) scarce, (+ +) fair, (+ + +) good, (NE) not evaluated.

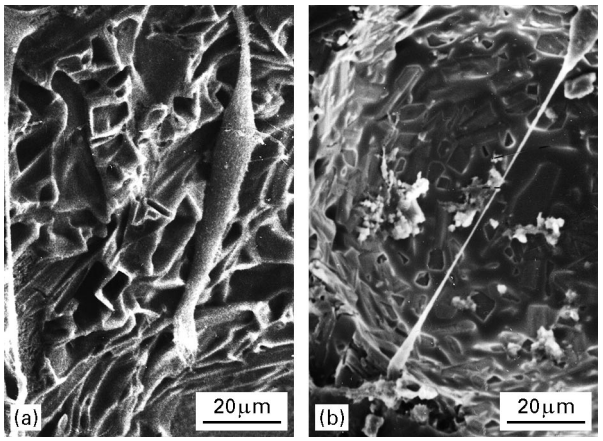

Figure 1 SEM micrographs showing (a) elongated fibroblasts cultured on AP40, and (b) cell culture on RKKP showing elongated fibroblasts growing on the porosity of the *biological glass.*

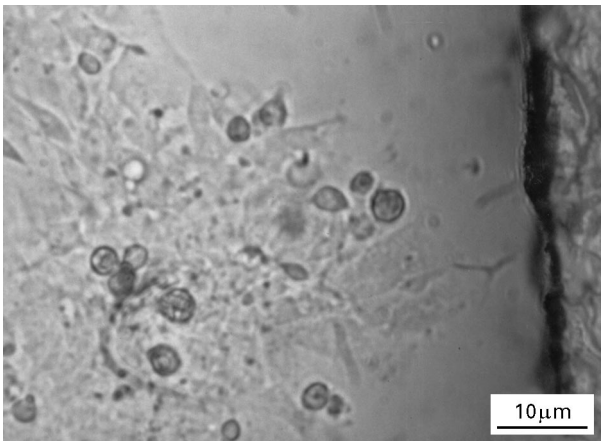

Figure 2 Osteoblast cultured in the presence of RKKP (phase-contrast light microscopy).

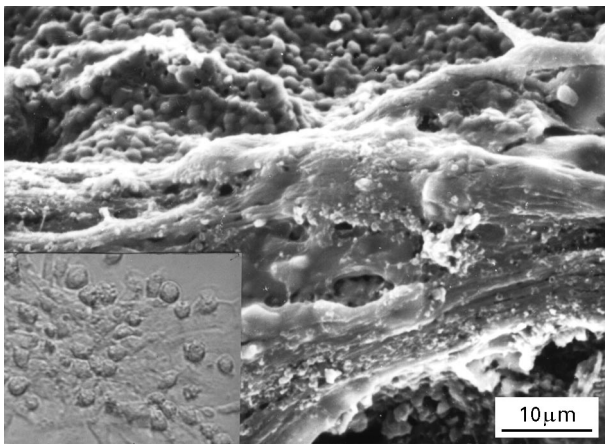

Figure 3 Fibroblasts cultured on HA (SEM). Inset: osteoblast cultured on HA (phase-contrast light microscopy).

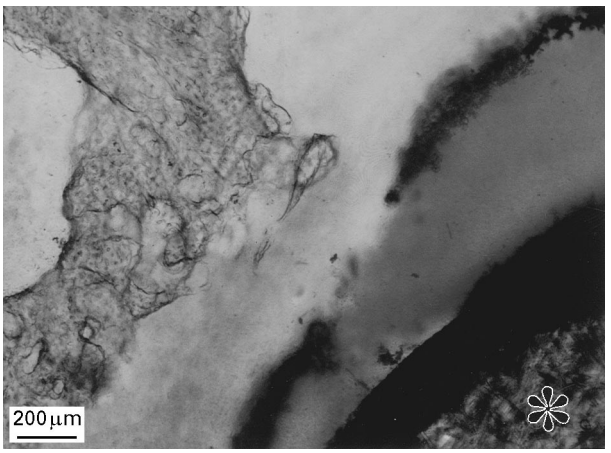

Figure 4 AP40 (*) implanted in OVX rat showing a quite homogeneous structure. Fibrotic reaction can be observed round the implant (semithin section, toluidine blue).

the implanted nails are listed in Table III. The differences in composition between the implant and the as-produced material can be obtained comparing Tables III and I. Variations of less than 2% were probably due to constraint to 100% of the semiquantitative analysis. For both glasses, in the INT group P concentrations increased considerably, whereas those of Na, Mg and K decreased. The only exception was Ca, which remained virtually unchanged with AP40, and declined slightly with RKKP. In OVX rats, P concentrations increased less than in normal rats, while Na and Mg decreased more than in normal rats. A marked but opposite trend was observed for Ca, which increased with AP40 and decreased with RKKP.

Table IV reports the results of the microanalyses performed on the bone surrounding the implants. The Ca : P ratios calculated on the basis of these data (Table V) demonstrate a considerable difference in the behaviour of the biological glasses in the two groups. The deposited layer around the samples of INT rats had a Ca : P ratio of 1.5. This stoichiometric value could be attributed to $Ca_3(PO_4)_2$ (TCP) or more probably to a calcium-deficient apatite (CDA) i.e. $Ca_9H(PO_4)_6(OH)$, coming from a solid solution between HA and DCP ($CaHPO_4$). Surprisingly, in OVX rats the deposited layer seems to be an exact HA-like compound (Ca : P atomic ratio of 1.7). This small higher ratio could also be attributed to some $CaCO_3$ composites, such as $Ca_{5+x}(PO_4)_3(CO_3)_xOH$ (which is the real apatitic compound of bone), with a very low stoichiometric index, $x = 0.1$.

3.2.2. HA

Upon morphological analysis, the cells of the bone tissue around the implant showed aspects of active metabolism, thus suggesting an active osteoinductive process. The areas of bone–implant contact were numerous in INT and scarce in OVX rats (Figs 8 and 9).

Microanalysis evidenced no significant differences between INT and OVX rats at the centre of the implant (Table II) or compared with the as-produced composition (Table I). This confirms the greater stability of Ca-phosphate ceramics compared with biological glasses, even though these data need to be substantiated by mechanical-stability and long-term load-bearing condition tests. The Ca : P atomic ratios deduced from the data of Table III are reported in Table IV. On the basis of the above-mentioned

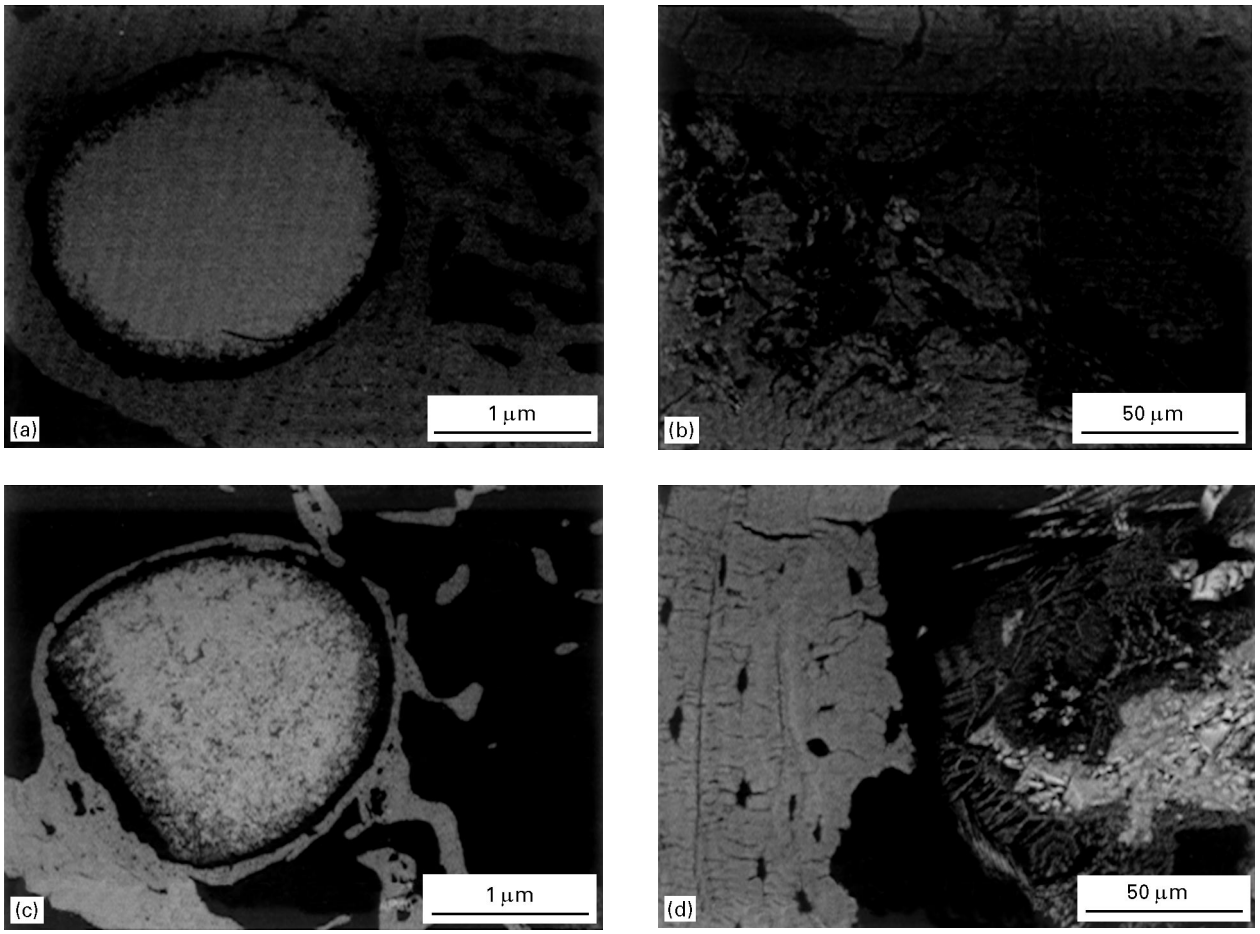

Figure 5 SEM micrograph of AP40 implant in normal (a, b) and osteoporotic (c, d) rat.

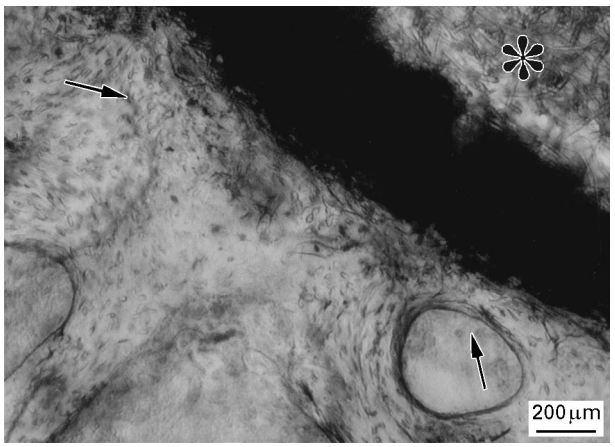

Figure 6 RKKP (*) implanted in osteoporotic rat displaying features of osteoinduction (→) (semithin section, toluidine blue).

considerations, in both INT and OVX rats the high Ca : P ratios (1.8 and 1.7, respectively) could be attributed to a $Ca_{5+x}(PO_4)_3(CO_3)_xOH$ compound with a very low stoichiometric index, x ($x = 0.1$ for OVX, $x = 0.2$ for INT).

3.2.3. CcHA

Sections from CcHA implants exhibited an evident mesenchymal reaction between bone and implant with several features of osteoinduction. Bone trabeculae penetrating the HA implant were also observed (Fig. 10).

3.2.4. DCMC–CaP

The microscopic analysis of histological samples coming from implantation on sheep showed a clear difference between the reparative-reconstitutive bone tissue obtained with and without chitosan. First, the cells were more numerous in treated legs than in control legs, and their large size and star-shape were suggestive of activation. Second, and most important, a wide osteogenic reaction (Fig. 11) moved from the rim of the surgical lesion towards its centre. The surgical hole was completely filled and at its core there was only mesenchymal-type tissue irregularly bordered with neoformed trabeculae. In control legs, dense fibrous tissue invaded the surgical lesion, and a central coagulum was sometimes observed. Elongated cells were inserted into a collagen network, but there were no features of vascularization. The external boundary of the hole exhibited a sudden transition from the fibrous reparative-reconstitutive tissue and the bone. The latter showed scarce signs of tissue remodelling (Fig. 12).

4. Discussion

The application of bioactive ceramic coatings to prostheses aims to confer strength to a material that exerts beneficial effects on bone-tissue growth but lacks itself the toughness and stability required of an implant device. Strength, however, is crucial, as the coating transfers the stress from the prosthesis to the

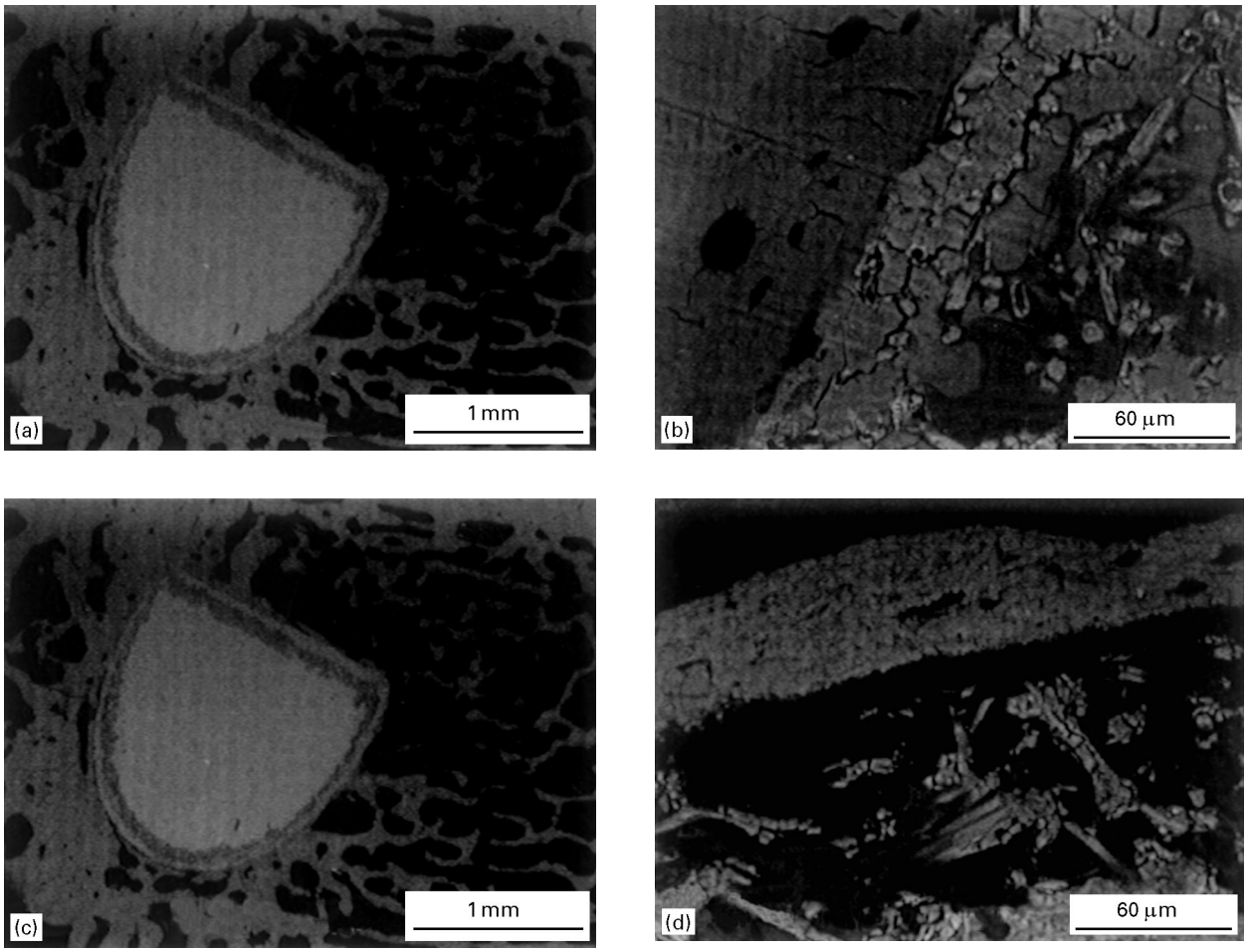

Figure 7 SEM micrograph of RKKP implant in normal (a, b) and osteoporotic (c, d) rat.

TABLE III Microanalysis of the nail cores following implantationin rats (values expressed as wt %, standard deviation = ± 5%)

	AP40	RKKP	HA
INT			
Ca	45.00	42.1	69.8
P	13.2	12.8	30.2
Si	37.9	38.8	–
Na	1.5	1.4	–
Mg	1.8	1.8	–
K	0.6	0.7	–
La	–	0.8	–
Ta	–	0.8	–
OVX			
Ca	47.3	41.5	69.5
P	9.7	10.4	30.5
Si	41.1	40.9	–
Na	0.2	1.1	–
Mg	0.7	1.2	–
K	1.0	1.4	–
La	–	1.3	–
Ta	–	1.4	–

TABLE IV Microanalysis of the bone surrounding the implant in rats (values expressed as wt %, standard deviation = ± 5%)

	AP40	RKKP	HA
INT			
Ca	65.2	64.0	68.4
P	33.3	33.4	30.1
Na	0.3	0.4	0.5
Mg	0.1	0.1	0.8
OVX			
Ca	67.8	67.8	67.7
P	30.4	30.0	30.8
Na	0.5	0.4	0.5
Mg	0.4	0.3	0.6

TABLE V Ca/P atomic ratios calculated from the values of Table IV

Rats	AP40	RKKP	HA
INT	1.5	1.5	1.8
OVX	1.7	1.7	1.7

surrounding tissue. The metal–ceramic coating interface is thus critical, depending as it does on the strength of the ceramic. Conversely, when the ceramic coating is used to enhance bone-tissue formation around and into the prosthetic surface, thereby helping to establish a mechanical form of retention, the interface loses its central importance and the ceramic needs to be endowed with the properties that enhance bone-tissue ingrowth immediately after surgery [13].

The rate of bioactivity is related to the chemical reactivity of the material and causes interface dissolution, precipitation and ion exchange reactions. It also appears to depend on a substrate function affecting collagen deposition and cell differentiation and

proliferation [14]. This was particularly evident in the biological glasses in our *in vivo* tests. The similar chemical rearrangement observed in both glasses suggests that these materials undergo modifications directly dependent on the biological environment, with initial release towards the bone of phosphorous, alkaline and alkaline-earth ions, as already well known [15]. Careful control of the composition (chemical modifications occur to a depth of about 400–500 μm) makes biological glass suitable also for an osteoporotic environment. The reasons for the different behaviour observed in osteoporotic bone are unknown, although the different rates of ionic exchange observed in our samples confirm the existence in healthy and osteoporotic bones of different biochemical mechanisms (compare Tables I, III–V). A surprising finding was the different Ca : P atomic ratios detected in the bone surrounding the implants: it could correspond to a calcium-deficient HA (CDA) in healthy subjects and to HA in osteoporotic subjects.

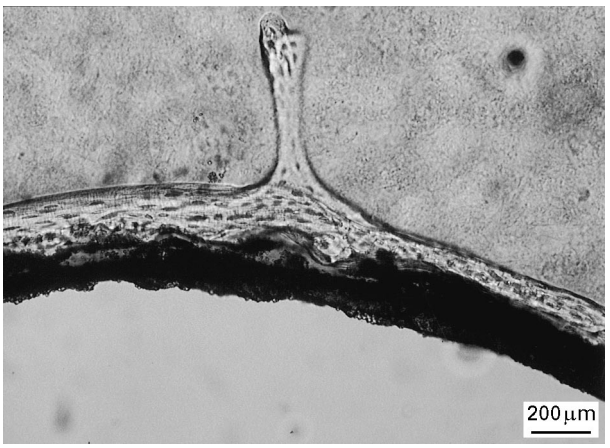

Figure 8 HA nails implanted in osteoporotic rat showing the presence of neoformed bone (semithin section, toluidine blue).

HA is widely used as a bone substitute for the repair of bone defects. As the HA compounds may differ in sintering temperature, however, they may exhibit differences in their *in vitro* dissolution features and *in vivo* performance [16]. However, the microstructure of HA, which consists of roundish, densely packed grains, differs from that of the HA microcrystals found in bone, which are needle-shaped and interconnected with collagen fibres. On the other hand, HA is thermodynamically stable in the bone and in bone-like environments, and also in its ceramic form; it is therefore recognized by the cells as a natural biological material, suitable as a substrate: indeed, it does not release ions or prime any biochemical activity, although it may undergo weak chemical carbonatation on the surface.

The *in vivo* tests of the present study suggest that the bioactivity of ceramic substrates can be enhanced by chitosan. The poor cell growth observed *in vitro* on CcHA implants may be partially attributed to a high dissolution rate that undermined cell adhesion and proliferation; moreover, the absence in the *in vitro* tests of extracellular factors, which are essential for cell

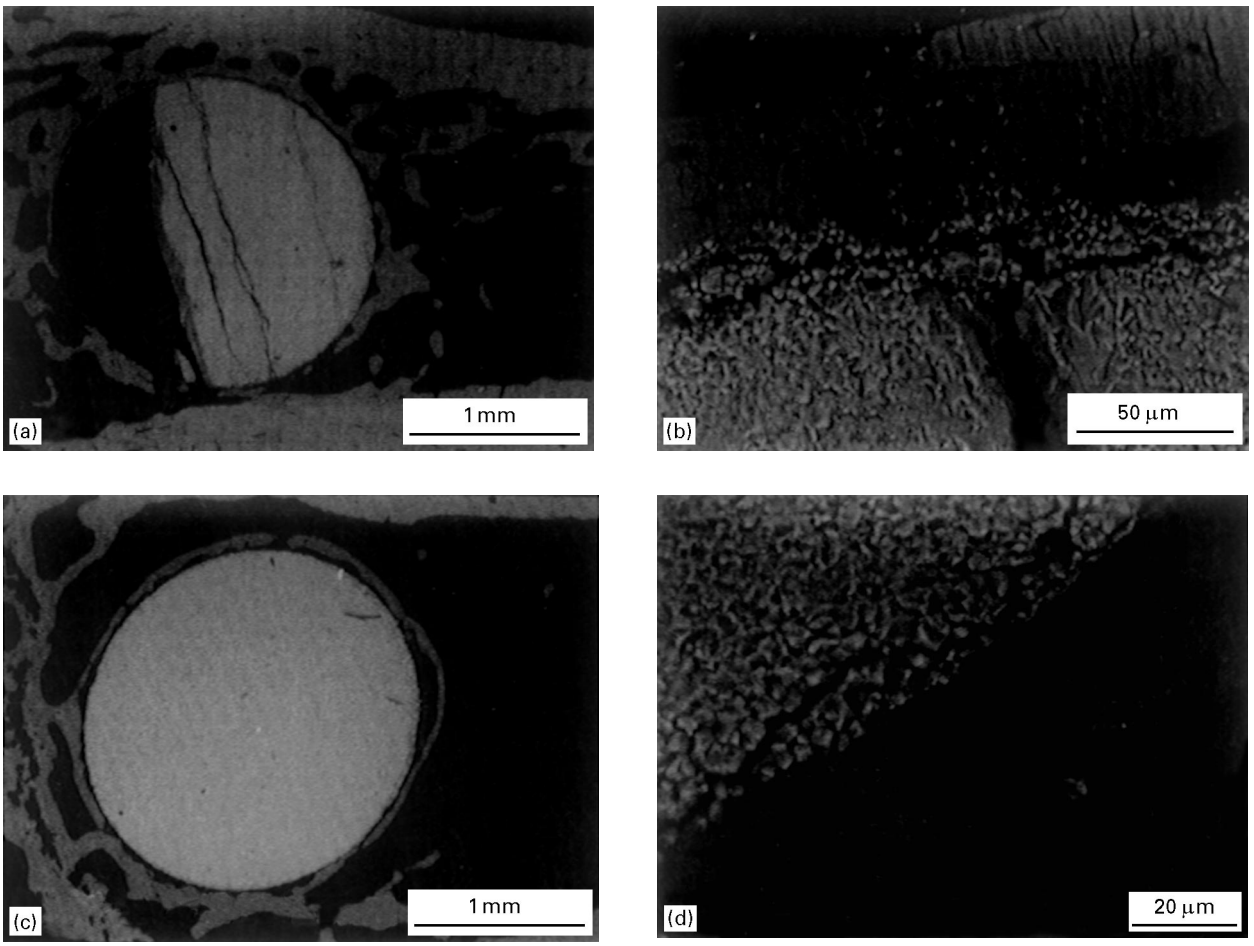

Figure 9 SEM micrograph of HA implant in normal (a, b) and osteoporotic (c, d) rat.

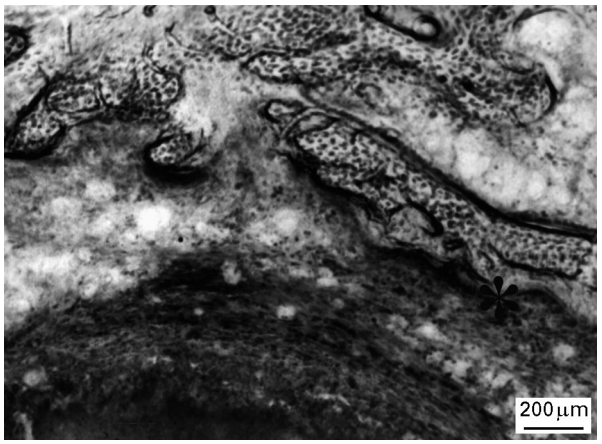

Figure 10 CcHA implant showing stromal reaction (*) between bone and implant (rabbit) (semithin section, toluidine blue).

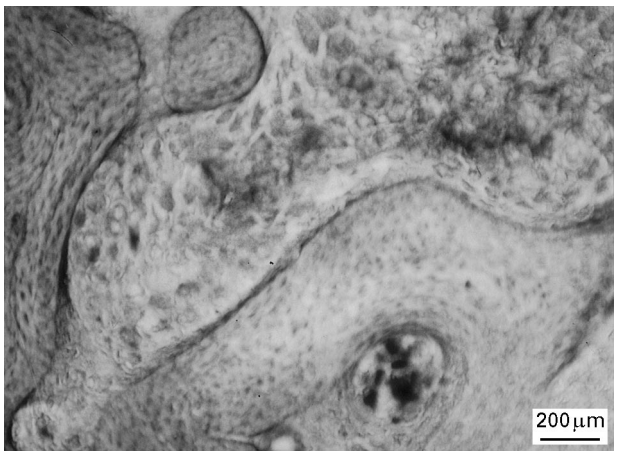

Figure 11 DCMC–CaP-treated sheep leg exhibiting osteogenesis (semithin section, toluidine blue).

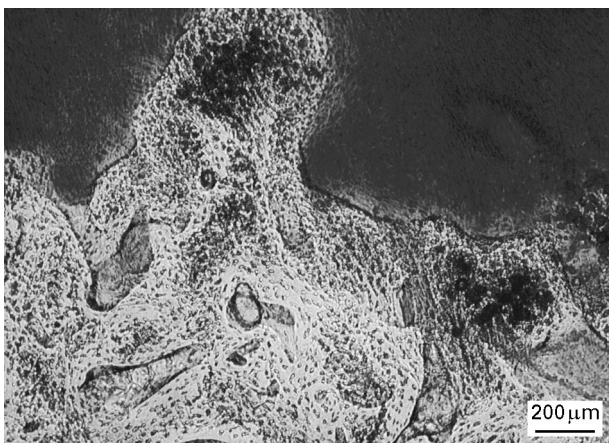

Figure 12 Control femoral condyle in sheep showing scarce tissue remodelling and a central blood coagulum (semithin section, toluidine blue).

behaviour, does not allow DCMC to perform its biological role. This suggests that future *in vitro* tests should be conducted in parallel with *in vivo* tests. In osteoporotic patients, bioresorbable ceramics could also incorporate therapeutic compounds such as bisphosphonate to enhance the osteointegration of the prosthesis. In the future, we intend to study whether the data obtained with ceramics can be obtained also with different mesenchymal cell lines.

Acknowledgements

The authors are grateful to Merck Clevenot (Nogent-sur-Marne, France) for supplying the crustacean chitosan manufactured by Aber Technologies (Plovien, France), to Gentili S.p.A. (Pisa, Italy) for the generous collaboration in obtaining soft and spongy hydrophilic DCMC associated with calcium and phosphate (DCMC–CaP), and to Braxel S.p.A. (Ancona, Italy) for helpful suggestions.

References

1. W. S. PIETRZAK, D. SARVER and M. VERSTYNEN, *Bone* **19** (supplement) (1996) 190S.
2. A. LEUTENEGGER, *Helv. Chim. Acta* **60** (1994) 1061.
3. D. A. BRUSHINSKI, N. E. SESSLER, R. E. GLENA and J. D. FEATHERSTONE, *J. Bone Miner. Res.* **9** (1994) 213.
4. M. D. BENAHAMMED, D. HEYMANN, M. BERREUR, M. COTTREL, A. GODARD, G. DACULSI and G. PRADAL, *J. Histochem. Cytochem.* **44** (1996) 1131.
5. J. L. ONG, K. K. CHUTUR and L. C. LUCAS, *J. Biomed. Mater. Res.* **28** (1994) 1337.
6. C. J. DAMIEN, J. L. RICCI, P. CHRISTEL, H. ALEXANDER and J. L. PATAT, *Calcif. Tissue Int.* **55** (1994) 151.
7. R. A. A. MUZZARELLI, C. ZUCCHINI, C. ESPOSITO, P. ILARI, A. PUGNALONI, M. MATTIOLI BELMONTE, G. BIAGINI and C. CASTALDINI, *Biomaterials* **14** (1993) 925.
8. M. MATTIOLI BELMONTE, R. A. A. MUZZARELLI and B. MUZZARELLI, *Carbohydrates in Europe* **19** (1997) 30.
9. M. TORIYAMA, A. RAVAGLIOLI, A. KRAJEWSKI, C. GALASSI, E. RONCARI and A. PIANCASTELLI, *J. Mater. Sci.* **30** (1995) 3216.
10. A. KRAJEWSKI, G. C. CELOTTI, A. RAVAGLIOLI and M. TORIYAMA, *Cryst. Res. Technol.* **31** (1996) 637.
11. M. TORIYAMA, A. RAVAGLIOLI, A. KRAJEWSKI, G. C. CELOTTI and A. PIANCASTELLI, *J. European Ceram.* **16** (1996) 429.
12. R. A. A. MUZZARELLI, P. ILARI and M. PETRARULO, *Int. J. Biol. Macromol.* **16** (1994) 177.
13. P. DUCHENEY and J. M. CUCKLER, *Clin. Orthop.* **276** (1992) 102.
14. G. DACULSI and J. P. LEGEROS, *J. Biomed. Mater. Res.* **31** (1996) 495.
15. A. RAVAGLIOLI and A. KRAJEWSKI (eds) "Bioceramics: materials, properties and applications" (Chapman & Hall, London, 1992).
16. T. KITSUGI, T. NAKAMURA, M. OKA, Y. SENAHA, T. GOTO and T. SHIBUYA, *J. Biomed. Mater. Res.* **30** (1996) 261.

Received 7 January
and accepted 26 January 1998